

## Variable-Dilation Embeddings of Hypercubes into Star Graphs: Performance Metrics, Mapping Functions, and Routing

Marcelo Moraes de Azevedo<sup>\*1</sup>, Nader Bagherzadeh<sup>1</sup>, and Shahram Latifi<sup>2</sup>

<sup>1</sup> Dept. of Elec. & Comp. Engr. – Univ. of Calif. – Irvine, CA 92717

<sup>2</sup> Dept. of Elec. & Comp. Engr. – Univ. of Nevada – Las Vegas, NV 89154

**Abstract.** We present load 1 embeddings of a  $k$ -dimensional hypercube  $Q_k$  into an  $n$ -dimensional star graph  $S_n$ . Dimension  $i$  links of  $Q_k$  are mapped into paths of length at most  $d_i$  in  $S_n$ , where  $d_i$  varies with  $i$  rather than being fixed. Our embeddings are an attractive alternative to previously known techniques, producing small *average dilation* and small *average congestion* without sacrificing expansion. We provide a thorough characterization of our embeddings, which spans several combinations of node mapping functions and routing algorithms in  $S_n$ .

### 1 Introduction

The star graph [1] is regarded as an attractive network for parallel processing, featuring smaller degree and diameter than a hypercube [5] of comparable size. However, the repertory of star graphs algorithms is still small compared to that of the hypercube. In this paper, we investigate load 1 embeddings of  $Q_k$  into  $S_n$ , which can be used to port algorithms developed for the hypercube to a star graph. Previous work on this problem sought to minimize *dilation* and *expansion*, but has produced embeddings for which a trade-off between these metrics exists [7]. The difficulty in minimizing dilation and expansion is due to topological differences between the two networks (e.g., degree and minimum cycle length) [7]. Moreover, previous research on embeddings of  $Q_k$  into  $S_n$  has not addressed some important performance metrics, which are discussed in this paper. These include *average dilation*, *congestion*, and *average congestion*. The average dilation and average congestion metrics are good approximations for the communication slowdown induced by an embedding, and are often correlated. In particular, average dilation has been used as a standard performance metric in practical evaluations of embedding heuristics into hypercubes [4].

We present *variable-dilation embeddings (VDEs)* which consistently achieve small average dilation and small average congestion (e.g., one of our VDE techniques produces values for these metrics respectively in the ranges [1.50, 3.24] and [1.00, 3.21], for  $n : 4 \rightarrow 10$ ). Simultaneously, the expansion of our VDEs matches that achieved by dilation 4 embeddings of [7]. Another advantage which stems

---

\* This research is supported in part by CNPq, Brazil, under the grant No. 200392/92-1.

from our techniques include the capability of employing unused nodes in  $S_n$  (up to 100% capacity) to host additional VDEs (see [2] for more on this topic).

Using several performance metrics which are defined in Sec. 2, and a combination of mathematical analysis and computer simulation, we provide a thorough characterization of our VDEs. Metrics which are derived analytically include expansion, dilation, and dilation along each of the hypercube dimensions. Average dilation, average congestion, and congestion are computed with a custom simulation program, which supports all of the VDEs presented in this paper. Measures for these last three metrics were computed over a selection of four different *node mapping functions* (NMFs), and four different routing algorithms in  $S_n$ . The paper illustrates some of the measures we obtained, pointing out the most promising combinations of NMFs and routing algorithms.

## 2 Variable-Dilation Embeddings (VDEs)

**Performance Metrics: Definitions.** Let  $G_k = \{V(G_k), E(G_k)\}$  be a hierarchical  $k$ -dimensional graph, such that  $G_{k+1}$  is obtained recursively from  $c(k)$  many copies of  $G_k$ . We refer to the links connecting the  $c(k)$  copies of  $G_k$  that exist within  $G_{k+1}$  as *dimension  $(k+1)$  links*.

An *embedding* of  $G_k$  into  $H_n$ , which we denote by  $f : G_k \mapsto H_n$ , is a mapping of  $V(G_k)$  into  $V(H_n)$  and of  $E(G_k)$  into paths of  $H_n$ . In this paper,  $f$  is uniquely specified by a *node mapping function* (NMF)  $f_V : V(G_k) \mapsto V(H_n)$  and a *deterministic routing algorithm*  $r_H$  of  $H_n$ . Thus, a link  $(u, v)$  of  $G_k$  is mapped to a path  $f(u, v) = r_H(f_V(u), f_V(v))$ .

The *node image* of  $f$  is  $f(V(G_k)) = \{f_V(u) : u \in V(G_k)\}$ . The *load* of  $f$ , denoted by  $\lambda(f)$ , is the maximum number of nodes of  $G_k$  that are mapped to any single node of  $H_n$ . The *dilation* of  $f$  is  $d(f) = \max\{\text{dist}_H(f_V(u), f_V(v)) : (u, v) \in E(G_k)\}$ , where  $\text{dist}_H(x, y)$  is the distance in  $H_n$  between two vertices  $x$  and  $y$  of  $H_n$ . The *expansion* of  $f$  is  $X(f) = |V(H_n)|/|V(G_k)|$ .

Let  $E_i(G_k)$  denote the subset of dimension  $i$  links in  $E(G_k)$ . The *dilation of  $f$  along the  $i^{\text{th}}$  dimension of  $G_k$*  is  $d_i(f) = \max\{\text{dist}_H(f_V(u), f_V(v)) : (u, v) \in E_i(G_k)\}$ . Hence,  $d(f) = \max\{d_i(f) : 1 \leq i \leq k\}$ .  $f$  is a *variable-dilation embedding* (VDE) if  $d_i(f) < d(f)$ , for at least one dimension  $i$  of  $G_k$ . Accordingly,  $f$  is a *fixed-dilation embedding* if  $d_i(f) = d(f)$ ,  $\forall i$ ,  $1 \leq i \leq k$ . The *dilation vector* of  $f$  is  $\overline{d}(f) = [d_1(f), d_2(f), \dots, d_k(f)]$ . The *average dilation* of  $f$  is  $d_{avr}(f) = \left(\sum_{(u,v) \in E(G_k)} \text{dist}_H(f_V(u), f_V(v))\right) \cdot (|E(G_k)|)^{-1}$ .

Let  $(u, v)$  and  $(x, y)$  be links of  $G_k$  and of  $H_n$ , respectively. The congestion induced by  $(u, v)$  into  $(x, y)$ , denoted by  $cg_{(x,y)}(f(u, v))$ , is 1 if  $f(u, v)$  traverses  $(x, y)$ , and 0 otherwise. The congestion induced by  $f$  into  $(x, y)$  is  $cg_{(x,y)}(f) = \sum_{(u,v) \in E(G_k)} cg_{(x,y)}(f(u, v))$ . The *congestion* of  $f$  is  $cg(f) = \max\{cg_{(x,y)}(f) : (x, y) \in E(H_n)\}$ . The *congestion induced by dimension  $i$  links* of  $G_k$  into  $H_n$  is  $cg(f(E_i(G_k))) = \max\{\sum_{(u,v) \in E_i(G_k)} cg_{(x,y)}(f(u, v)) : (x, y) \in E(H_n)\}$ . The *link image* of  $f$  is  $f(E(G_k)) = \{(x, y) \in E(H_n) : cg_{(x,y)}(f) \geq 1\}$ . The *average congestion* of  $f$  is  $cg_{avr}(f) = \left(\sum_{(x,y) \in f(E(G_k))} cg_{(x,y)}(f)\right) \cdot (|f(E(G_k))|)^{-1}$ .

**The Guest Graph.** A  $k$ -dimensional hypercube graph  $Q_k$  contains  $2^k$  nodes, which are labeled with binary strings of length  $k$ . A node  $\phi = q_1 \dots q_i \dots q_k$  is connected to  $k$  distinct nodes, respectively labeled with strings  $\phi_i = q_1 \dots \bar{q}_i \dots q_k$ ,  $1 \leq i \leq k$ , where  $\bar{q}_i$  denotes the binary negation of bit  $q_i$  [5]. The link connecting  $\phi$  and  $\phi_i$  is a *dimension  $i$  link* of  $Q_k$ .

**The Host Graph.** An  $n$ -dimensional star graph  $S_n$  contains  $n!$  nodes which are labeled with the  $n!$  possible permutations of  $n$  distinct symbols. In this paper, we use the integers  $\{1, 2, \dots, n\}$  to label the nodes of  $S_n$ . A node  $\pi = p_1 \dots p_i \dots p_n$  is connected to  $(n - 1)$  distinct nodes, respectively labeled with permutations  $\pi_i = p_i \dots p_{i-1} p_{i+1} \dots p_n$ ,  $2 \leq i \leq n$  [1]. The link connecting  $\pi$  and  $\pi_i$  is a *dimension  $i$  link* of  $S_n$ .

**The Intermediary Graph.** Our embeddings of  $Q_k$  into  $S_n$  use an  $(n - 1)$ -dimensional mesh of size  $2 \times 3 \times \dots \times n$  as an intermediary reference graph. We denote such a graph by  $M_{n-1}$ , and label its nodes with  $(n - 1)$ -integer vectors  $m_1 \dots m_i \dots m_{n-1}$ , where  $0 \leq m_i \leq i$ . A node  $\omega = m_1 \dots m_i \dots m_{n-1}$  is connected to at most  $2n - 3$  distinct nodes, respectively labeled with vectors  $\omega_i^- = m_1 \dots (m_i - 1) \dots m_{n-1}$  and  $\omega_i^+ = m_1 \dots (m_i + 1) \dots m_{n-1}$ ,  $1 \leq i < n$ .  $\omega_i^-$  ( $\omega_i^+$ ) is a *left (right) dimension  $i$  neighbor* of  $\omega$  if  $\omega_i^-$  ( $\omega_i^+$ ) exists.

**NMFs  $g_V : V(M_{n-1}) \mapsto V(S_n)$ .** Our embeddings of  $Q_k$  into  $S_n$  use two-step NMFs. Initially, we employ an NMF  $h_V : V(Q_k) \mapsto V(M_{n-1})$ . The second step uses an NMF  $g_V : V(M_{n-1}) \mapsto V(S_n)$ . The composite NMF  $f_V : V(Q_k) \mapsto V(S_n)$  is denoted by  $f_V = h_V \odot g_V$ .

In what follows, we describe four different NMFs  $g_V : V(M_{n-1}) \mapsto V(S_n)$ , which we denote by  $g_V^{nonh}$ ,  $g_V^{mnonh}$ ,  $g_V^{hier}$ , and  $g_V^{qhier}$ . These NMFs are respectively referred to as the *non-hierarchical NMF* [6, 8], the *modified non-hierarchical NMF* [2], the *hierarchical NMF*, and the *quasi-hierarchical NMF*. All four NMFs embed  $M_{n-1}$  into  $S_n$  with load 1, expansion 1, and dilation 3. The dilation vectors of the embeddings produced by  $g_V^{nonh}$ ,  $g_V^{mnonh}$ ,  $g_V^{hier}$ , and  $g_V^{qhier}$  are respectively  $\underbrace{[3, \dots, 3, 1]}_{n-2}$ ,  $\underbrace{[3, \dots, 3]}_{n-1}$ ,  $\underbrace{[1, 2, 3, \dots, 3]}_{n-3}$ , and  $\underbrace{[3, 2, 3, \dots, 3]}_{n-3}$ .

Let  $\pi$  be a permutation of  $n$  symbols. We denote the transposition of *symbols*  $i$  and  $j$  in  $\pi$  by  $(i j)_s$ . Similarly, we denote the transposition of the symbols occupying the  $i^{th}$  and the  $j^{th}$  *positions* in  $\pi$  by  $(i j)_p$ . We define an operator  $\circ$  which applies transpositions to permutations. Hence,  $2413 \circ (2 4)_s = 4213$ , and  $2413 \circ (2 4)_p = 2314$ . NMFs  $g_V^{nonh}$ ,  $g_V^{mnonh}$ ,  $g_V^{hier}$ , and  $g_V^{qhier}$  can be generically described by the algorithm depicted in Table 1. For example,  $g_V^{mnonh}(102) = 2134 \circ (4 3)_p \circ (3 2)_p = 2413$ .

**NMF  $h_V : V(Q_k) \mapsto V(M_{n-1})$ .** In what follows, we present an NMF  $h_V : V(Q_k) \mapsto V(M_{n-1})$ , which is common to all of our VDEs. We denote the corresponding composite NMFs  $f_V : V(Q_k) \mapsto V(S_n)$  by  $f_V^{nonh} = h_V \odot g_V^{nonh}$ ,  $f_V^{mnonh} = h_V \odot g_V^{mnonh}$ ,  $f_V^{hier} = h_V \odot g_V^{hier}$ , and  $f_V^{qhier} = h_V \odot g_V^{qhier}$ .

Let  $F(x, y) = x(y + 1) - 2^{x+1} + 2$ , and let  $n$ ,  $\ell$ , and  $k$  be integers such that  $n \geq 4$ ,  $2 \leq \ell \leq \lceil \log_2 n \rceil$ , and  $F(\ell - 1, n) < k \leq F(\ell, n)$ . Let  $\phi[\ ]$  and  $\omega[\ ]$  be nodes of  $Q_k$  and  $M_{n-1}$ , respectively. An algorithmic description of  $h_V$  follows:

**Table 1.** Algorithmic description for NMFs  $g_V : V(M_{n-1}) \mapsto V(S_n)$

a. Choose an initial permutation $\pi_0$ from Table 1a, according to the type of NMF $g_V$ and mesh coordinates $m_1 m_2$ .						
NMF	$m_1 m_2 = 00$	$m_1 m_2 = 10$	$m_1 m_2 = 01$	$m_1 m_2 = 11$	$m_1 m_2 = 02$	$m_1 m_2 = 12$
$g_V^{nonh}$	12345 ... n	12435 ... n	13245 ... n	13425 ... n	14235 ... n	14325 ... n
$g_V^{mnonh}$	12345 ... n	21345 ... n	13245 ... n	23145 ... n	31245 ... n	32145 ... n
$g_V^{hier}$	12345 ... n	21345 ... n	31245 ... n	13245 ... n	23145 ... n	32145 ... n
$g_V^{qhier}$	12345 ... n	21345 ... n	23145 ... n	13245 ... n	32145 ... n	31245 ... n

b. For $i : 3 \rightarrow (n - 1)$ , apply the first $m_i$ transpositions specified for dimension $i$ and NMF $g_V$ in Table 1b to $\pi_0$ .				
NMF	$i = 3$	$i = 4$	...	$i = n - 1$
$g_V^{nonh}$	$(1\ 2)_s \circ (2\ 3)_s \circ (3\ 4)_s$	$(1\ 2)_s \circ \dots \circ (4\ 5)_s$	...	$(1\ 2)_s \circ \dots \circ (n - 1\ n)_s$
$g_V^{mnonh}$	$(4\ 3)_p \circ (3\ 2)_p \circ (2\ 1)_p$	$(5\ 4)_p \circ \dots \circ (2\ 1)_p$	...	$(n\ n - 1)_p \circ \dots \circ (2\ 1)_p$
$g_V^{hier}, g_V^{qhier}$	$(4\ 3)_s \circ (3\ 2)_s \circ (2\ 1)_s$	$(5\ 4)_s \circ \dots \circ (2\ 1)_s$	...	$(n\ n - 1)_s \circ \dots \circ (2\ 1)_s$

for  $(i = 1; i < n; i++) \omega[i] = 0;$   
 for  $(e = 1; F(e - 1, n) < k; e = e + 1)$   
 for  $(i = F(e - 1, n) + 1; i \leq \min(F(e, n), k); i = i + 1)$   
 $\omega[i - F(e - 1, n) + 2^e - 2] = \omega[i - F(e - 1, n) + 2^e - 2] + 2^{e-1} \cdot \phi[i];$

Table 2 depicts the VDE  $h : Q(4) \mapsto M(3)$  produced by NMF  $h_V$ . Properties for  $h$  are  $X(h) = 1.5$ ,  $\lambda(h) = 1$ ,  $d(h) = 2$ ,  $\overline{d(h)} = [1, 1, 1, 2]$ , and  $d_{avr}(h) = 1.25$ . Also shown in Table 2 are VDEs  $f : Q(4) \mapsto S(4)$  produced by  $f_V^{nonh}$ ,  $f_V^{mnonh}$ ,  $f_V^{hier}$ , and  $f_V^{qhier}$ . The properties of  $f^{hier}$ , for example, are  $X(f^{hier}) = 1.5$ ,  $\lambda(f^{hier}) = 1$ ,  $d(f^{hier}) = 4$ ,  $\overline{d(f^{hier})} = [1, 2, 3, 4]$ , and  $d_{avr}(f^{hier}) = 2$ .

**Table 2.** Image nodes for NMFs  $h_V$ ,  $f_V^{nonh}$ ,  $f_V^{mnonh}$ ,  $f_V^{hier}$ , and  $f_V^{qhier}$  ( $n = k = 4$ )

NMF	Hypercube node ( $\phi$ )															
	0000	1000	0100	1100	0010	1010	0110	1110	0001	1001	0101	1101	0011	1011	0111	1111
$h_V$	000	100	010	110	001	101	011	111	002	102	012	112	003	103	013	113
$f_V^{nonh}$	1234	1243	1324	1342	2134	2143	2314	2341	3124	3142	3214	3241	4123	4132	4213	4231
$f_V^{mnonh}$	1234	2134	1324	2314	1243	2143	1342	2341	1423	2413	1432	2431	4123	4213	4132	4231
$f_V^{hier}$	1234	2134	3124	1324	1243	2143	4123	1423	1342	3142	4132	1432	2341	3241	4231	2431
$f_V^{qhier}$	1234	2134	2314	1324	1243	2143	2413	1423	1342	3142	3412	1432	2341	3241	3421	2431

**Properties of VDEs  $f : Q_k \mapsto S_n$ .** (see [3] for a proof).

**Theorem 1.** Let  $F(x, y) = x(y + 1) - 2^{x+1} + 2$ , and let  $n$ ,  $\ell$ , and  $k$  be integers such that  $n \geq 4$ ,  $2 \leq \ell \leq \lceil \log_2 n \rceil$ , and  $F(\ell - 1, n) < k \leq F(\ell, n)$ . Let  $f_V$  be one of the node mapping functions  $f_V^{nonh}$ ,  $f_V^{mnonh}$ ,  $f_V^{hier}$ , and  $f_V^{qhier}$ , and let  $f : Q_k \mapsto S_n$  be one of the corresponding embeddings  $f^{nonh}$ ,  $f^{mnonh}$ ,  $f^{hier}$ , and  $f^{qhier}$  generated by  $f_V$ . For each  $f$ , we define integers  $\gamma_i(f)$  as follows:

- $\gamma_i(f^{nonh}) = 0$  if  $i = F(e, n)$ ,  $\forall e \in [1, \ell]$ , and  $\gamma_i(f^{nonh}) = 2$  otherwise.
- $\gamma_i(f^{mnonh}) = 2$ ,  $\forall i$ .
- $\gamma_1(f^{hier}) = 0$ ,  $\gamma_2(f^{hier}) = 1$ , and  $\gamma_i(f^{hier}) = 2$ , for all  $i > 2$ .
- $\gamma_1(f^{qhier}) = 0$ ,  $\gamma_2(f^{qhier}) = 1$ , and  $\gamma_i(f^{qhier}) = 2$ , for all  $i > 2$ .

Then,  $\lambda(f) = 1$ ,  $X(f) = n!/2^k$ ,  $d(f) = \max_i \{d_i(f)\}$ , and:

$$\overline{d(f)} = \underbrace{[1 + \gamma_i(f), \dots, 2 + \gamma_i(f), \dots, \dots]}_{n-1}, \underbrace{[2 + \gamma_i(f), \dots, \dots]}_{n-3}, \underbrace{[2^{e-1} + \gamma_i(f), \dots, \dots]}_{F(e,n)-F(e-1,n)}, \underbrace{[2^{\ell-1} + \gamma_i(f), \dots]}_{k-F(\ell-1,n)}.$$

**Routing and Simulation Results.** We used simulation to characterize other important metrics of our VDEs, such as average dilation, average congestion, congestion, and congestion induced by dimension  $i$  links of  $Q_k$ . The tool supports all of the NMFs  $f_V^{nonh}$ ,  $f_V^{mnonh}$ ,  $f_V^{hier}$ , and  $f_V^{qhier}$ , and four deterministic routing algorithms in  $S_n$ . These algorithms are denoted by  $r_S^{can}$ ,  $r_S^{rcan}$ ,  $r_S^{ecan}$ , and  $r_S^{ocan}$ .

Recall that a link  $(u, v) \in E(Q_k)$  is mapped to a path  $f(u, v)$  in  $S_n$  with endpoints  $f_V(u)$  and  $f_V(v)$ . Let  $\pi_{u,v}$  denote the permutation which sorts  $f_V(u)$  into  $f_V(v)$ . Each routing algorithm employs a particular format for the *cyclic representation* of  $\pi_{u,v}$ , and executes  $\pi_{u,v}$  accordingly [3].  $r_S^{can}$ ,  $r_S^{rcan}$ ,  $r_S^{ecan}$ , and  $r_S^{ocan}$  represent  $\pi_{u,v}$  in *canonical format*, *reverse canonical format*, *even-only canonical format*, and *odd-only canonical format*, respectively [3].

Figure 1 depicts the average dilation and the average congestion produced by VDEs employing the combination  $f_V^{qhier} + r_S^{rcan}$ . Similar plots for other combinations of NMF and routing algorithm can be found in [3]. We consider the cases  $k : 2 \rightarrow 19$  and  $n : 4 \rightarrow 10$ , which correspond respectively to hypercubes of sizes  $4 \rightarrow 524, 288$ , and star graphs of sizes  $24 \rightarrow 3, 628, 800$ .  $f_V^{nonh}$ ,  $f_V^{mnonh}$ ,  $f_V^{hier}$ , and  $f_V^{qhier}$  achieve average dilation which lie in the ranges  $[2.25, 3.53]$ ,  $[2.00, 3.60]$ ,  $[1.50, 3.21]$ , and  $[1.50, 3.24]$ , respectively. Accordingly, measures for average congestion produced by the combinations  $f_V^{nonh} + r_S^{can}$ ,  $f_V^{mnonh} + r_S^{can}$ ,  $f_V^{hier} + r_S^{can}$ , and  $f_V^{qhier} + r_S^{can}$  lie in the ranges  $[1.00, 5.47]$ ,  $[1.19, 2.96]$ ,  $[1.07, 3.81]$ , and  $[1.00, 3.21]$ , respectively. Note that the average dilation computed for a VDE does not depend on the choice of routing algorithm.

Hierarchical NMFs achieve smaller average dilation than non-hierarchical NMFs, and produce smaller average congestion when used in combination with  $r_S^{rcan}$ . Conversely,  $r_S^{can}$  minimizes the average congestion produced by non-hierarchical NMFs. The combinations  $f_V^{mnonh} + r_S^{can}$  and  $f_V^{qhier} + r_S^{can}$  seem to be the most appropriate for star graphs employing canonical and reverse canonical routing, respectively.  $r_S^{ecan}$  and  $r_S^{ocan}$  produce congestion metrics which lie between the minima and maxima obtained with  $r_S^{rcan}$  ( $r_S^{can}$ ) and  $r_S^{can}$  ( $r_S^{rcan}$ ), when used in combination with hierarchical and non-hierarchical NMFs, respectively.

Several of our VDEs produce congestion 1 or 2 on the links of  $S_n$  when a single dimension of  $Q_k$  is used [3]. This is particularly important for algorithms which employ only a fraction of the links of  $Q_k$  at any point of their execution (e.g., SIMD algorithms). From the viewpoint of congestion, some interesting results are: 1)  $f_V^{mnonh} + r_S^{can}$  produces VDEs whose congestion is less than  $k$ , over the ranges  $k : 2 \rightarrow 19$  and  $n : 4 \rightarrow 10$ , and 2)  $f_V^{qhier} + r_S^{rcan}$  produces VDEs with congestion 1 when  $k \leq n - 1$  [3].

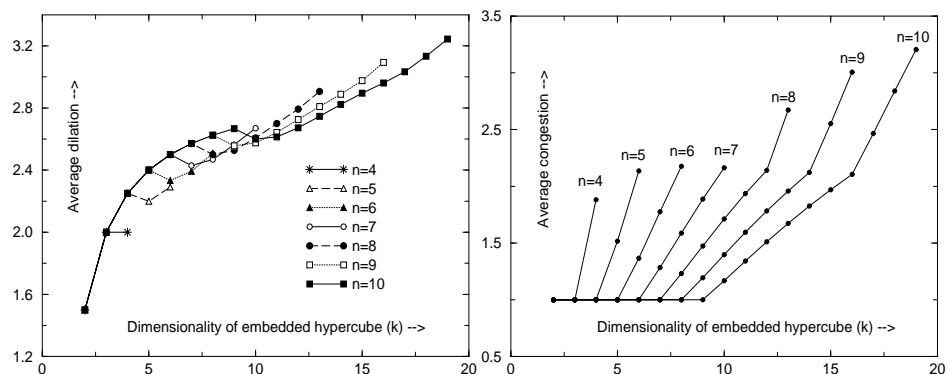


Fig. 1. Average dilation and average congestion produced by  $f_V^{ghier}$  and  $r_S^{rcan}$

### 3 Conclusion

This paper presented novel techniques for embedding a hypercube into a star graph. Our embeddings are designed for performance, and consistently produce small average dilation and small average congestion. We achieve these goals by employing variable-dilation embeddings, and a careful selection of node mapping functions and routing algorithms. Our techniques demonstrated the possibility of embedding large hypercubes into the star graph, with corresponding small expansion. On continued research, we are expanding our investigation on congestion metrics to a related technique introduced by the authors. Such a technique is referred to as *packing*, and can produce optimal expansion (i.e., 1) [2].

### References

1. Akers, S. B., Harel, D., Krishnamurthy, B.: The star graph: an attractive alternative to the  $n$ -cube. Proc. Int. Conf. Par. Proc. (1987) 393-400
2. Azevedo, M. M., Latifi, S., Bagherzadeh, N.: Low expansion packings and embeddings of hypercubes into star graphs. Proc. IEEE 15th Phoenix Conf. Comp. Comm. (1996) 115-122
3. Azevedo, M. M., Bagherzadeh, N., Latifi, S.: Variable-dilation embeddings of hypercubes into star graphs: performance metrics, mapping functions, and routing. Dept. Elec. & Comp. Engr. U. Cal., Irvine. Tech. Rep. ECE 96-05-01 (1996)
4. Chen, W.-K., Stallmann, M. F. M., Gehringer, E. F.: Hypercube embedding heuristics: an evaluation. Int. J. Par. Prog. **18** No. 6 (1989) 505-549
5. Hayes, J. P., Mudge, T.: Hypercube supercomputers. Proc. IEEE. **77** No. 12 (1989) 1829-1841
6. Jwo, J. S., Lakshminarayanan, S., Dhall, S. K.: Embedding of cycles and grids in star graphs. J. Circ., Sys., and Comp. **1** No. 1 (1991) 43-74
7. Nigam, M., Sahni, S., Krishnamurthy, B.: Embedding Hamiltonians and hypercubes in star interconnection networks. Proc. Int. Conf. Par. Proc. (1990) 340-343
8. Ranka, S., Wang, J.-C., Yeh, N.: Embedding meshes on the star graph. J. Par. Dist. Comp. **19** (1993) 131-135

This article was processed using the  $\text{\LaTeX}$  macro package with LLNCS style